Bone 58 (2014) 81–91

Contents lists available at ScienceDirect

Bone

journal homepage: www.elsevier.com/locate/bone

Original Full Length Article

Osteoblastic cell secretome: A novel role for progranulin during risedronate treatment

Milena Romanello [a,*], Elzbieta Piatkowska [b], Giulia Antoniali [c], Laura Cesaratto [c], Carlo Vascotto [c], Renato V. Iozzo [d], Daniela Delneri [b], Francesco L. Brancia [e]

[a] Laboratory of Regional Centre for Rare Diseases, University Hospital, Santa Maria della Misericordia, 33100 Udine, Italy
[b] Faculty of Life Sciences, University of Manchester, Manchester M13 9PT, UK
[c] Department of Biomedical Sciences and Technologies, University of Udine, 33100 Udine, Italy
[d] Department of Pathology, Anatomy and Cell Biology, Thomas Jefferson University, Philadelphia, PA, USA
[e] Aarhus University, Faculty of Agricultural Sciences, Aarhus, Denmark

ARTICLE INFO

Article history:
Received 3 July 2013
Revised 19 September 2013
Accepted 1 October 2013
Available online 11 October 2013

Edited by: Hong-Hee Kim

Keywords:
Bisphosphonates
Risedronate
Osteoblasts
Osteocytes
Progranulin
Differential proteomics

ABSTRACT

It is well established that osteoblasts, the key cells involved in bone formation during development and in adult life, secrete a number of glycoproteins harboring autocrine and paracrine functions. Thus, investigating the osteoblastic secretome could yield important information for the pathophysiology of bone. In the present study, we characterized for the first time the secretome of human Hobit osteoblastic cells. We discovered that the secretome comprised 89 protein species including the powerful growth factor progranulin. Recombinant human progranulin (6 nM) induced phosphorylation of mitogen-activated protein kinase in both Hobit and osteocytic cells and induced cell proliferation and survival. Notably, risedronate, a nitrogen-containing bisphosphonate widely used in the treatment of osteoporosis, induced the expression and secretion of progranulin in the Hobit secretome. In addition, our proteomic study of the Hobit secretome revealed that risedronate induced the expression of ERp57, HSP60 and HSC70, three proteins already shown to be associated with the prevention of bone loss in osteoporosis. Collectively, our findings unveil novel targets of risedronate-evoked biological effects on osteoblast-like cells and further our understanding of the mechanisms of action of this currently used compound.

Introduction

Osteoporosis is a skeletal disease characterized by low bone mass and microarchitectural deterioration of bone tissue due to an imbalance between bone resorption and bone formation, with a consequent increase in bone fragility and susceptibility to fracture. It has become a major medical problem in the last half century, largely as the result of an increased longevity and a changing lifestyle [1].

Bisphosphonates are synthetic analogs of inorganic pyrophosphate in which the oxygen atom bridging the two phosphates is replaced by a carbon atom; they are generally accepted as first-line therapy for osteoporosis because of their efficacy, safety, and ease of administration. They have a high affinity for calcium phosphate crystals, concentrate selectively in the skeleton, and decrease bone resorption. It has been reported that the chronic supply of nitrogen-containing bisphosphonates, such as alendronate, ibandronate, risedronate and zoledronate, significantly reduces the risk of vertebral fractures by 35–65% [2].

Bisphosphonates bound to bone hydroxyapatite are released under the acidic conditions present in the resorption lacunae leading to intracellular accumulation of the drugs. In the case of nitrogen-containing bisphosphonates, at the cellular level these compounds induce changes in the cytoskeletal structure of osteoclasts, reducing their resorption activity and promoting their apoptosis. This action is mainly caused by the inhibition of farnesyl pyrophosphate synthase (FPPS), an enzyme of the mevalonate biosynthetic pathway. FPPS is responsible for the formation of isoprenoid metabolites required for the prenylation of small GTPases that are important for cytoskeletal integrity and function of osteoclasts. In addition, the inhibition of FPPS by nitrogen-containing bisphosphonates leads to accumulation of isopentyl diphosphate (IPP), a metabolite immediately upstream of FPPS, which reacts with AMP to produce a new compound which also induces osteoclast apoptosis [3]. However, unlike their effects on osteoclasts, nitrogen-containing bisphosphonates promote osteoblast

Abbreviations: 2-DE, two-dimensional gel electrophoresis; ECL, enhanced chemiluminescence; FBS, fetal bovine serum; FPPS, farnesyl pyrophosphate synthase; IPP, isopentyl diphosphate; LC, liquid chromatography; MALDI-ToF, matrix-assisted laser desorption/ionization-time of flight; MS/MS, tandem mass spectrometry; MLO-Y4, murine long bone osteocyte-Y4; MTT, 3-(4,5-dimethylthiazol-2-yl)-2,5-diphenyltetrazolium bromide; PAGE, polyacrylamide gel electrophoresis; PMSF, phenylmethylsulfonyl fluoride; PVDF, polyvinylidene fluoride; SDS, sodium dodecyl sulfate; TFA, trifluoroacetic acid.

* Corresponding author.
E-mail address: romanello.milena@aoud.sanita.fvg.it (M. Romanello).

8756-3282/$ – see front matter © 2013 Elsevier Inc. All rights reserved.
http://dx.doi.org/10.1016/j.bone.2013.10.003

and osteocyte survival in vitro and in vivo, through the opening of connexin 43 hemichannels, followed by the activation of pro-survival MAPK cascade [4–6]. This pro-survival effect on cells of the osteoblastic lineage is exerted at concentrations ranging from 10^{-11} up to 10^{-6} M, which are several orders of magnitude lower than the ones required to inhibit osteoclast activity [7]. In addition, we have demonstrated that low doses of nitrogen-containing bisphosphonates promote the non-lytic release of ATP from human osteoblastic Hobit cell line in culture leading to autocrine activation of purinergic signaling through P2 nucleotide receptors and to upregulation of the molecular chaperone Hsp90 [8]. Regardless of the growing interest on the action of nitrogen-containing bisphosphonates on both osteoblasts and osteocytes, a more detailed picture of their effects at the molecular level is still missing.

We recently employed a label-free, shotgun proteomic approach to identify the protein species expressed by MLO-Y4 osteocytic cells [9]. Among the identified species we noticed that a secreted protein, i.e. progranulin (also known as PC cell derived growth factor, GRN or Acrogranin) [10], was increased upon low doses of the heterocyclic ring-containing risedronate treatment of MLO-Y4 cells [9]. Thus, we speculated that nitrogen-containing bisphosphonates may be involved in the modulation of bone cells secretome. Progranulin is a secreted glycoprotein that acts as an important regulator of wound repair, inflammation, cell growth, migration and transformation. It is overexpressed in a great variety of cancer cell lines and clinical specimens of breast, ovarian, and renal cancers as well as glioblastomas [11]. It has also been detected in the conditioned medium of mouse PC cells [12], human breast cancer [13] and multiple myeloma cells [14,15]. Progranulin interacts with the heparan sulfate proteoglycan perlecan and localizes in the basement membranes of tumor blood vessels suggesting a potential role in angiogenesis [16]. Moreover, progranulin appears to be an endogenous autocrine growth factor for urothelial cancer cells [17].

To provide a more comprehensive understanding of osteoblastic cell dynamics, we characterized the secretome of unstimulated Hobit osteoblastic-like cells and the role of risedronate on protein expression of osteoblasts-secreted proteins. To this end, we employed a proteomic approach combining one dimensional gel electrophoresis in gel digestion followed by micro and nanobore liquid chromatography (LC) tandem mass spectrometry (MS/MS) performed on protein samples obtained from conditioned medium of Hobit cells.

Materials and methods

Cell culture conditions and collection of conditioned medium

Culture media and antibiotics were purchased from Invitrogen (Carlsbad, CA). Hobit cells, a human osteoblast-like cell line immortalized with the SV40 T antigen was generously provided by Dr. Riggs, Mayo Foundation, Rochester, Minnesota. MLO-Y4 (murine long bone osteocyte-Y4) cells were kindly provided by Dr. L.F. Bonewald, Department of Oral Biology, School of Dentistry, University of Missouri, Kansas City, MO. Cells were cultured as already described [8,9], maintained at 37 °C in a 5% CO_2 atmosphere and grown to approximately 80% confluence in 150-mm^2 culture dishes (Sarsted, Verona, Italy). The cells were rinsed with serum-free medium at 37 °C, 3 times for 5 min and then incubated in the serum-free medium at 37 °C for 12 h or 24 h.

All the chemicals described below were from Sigma Aldrich Co. (Milan, Italy) unless otherwise specified. Risedronate was provided by Procter and Gamble Pharmaceuticals (Cincinnati, OH). Recombinant full-length human progranulin was purified essentially as described before with minor modifications [16]. Briefly, a pCEP-Pu vector bearing the sequence of the BM40 signal peptide and the full-length progranulin was electroporated into human embryonic kidney cells (293-EBNA) expressing the Epstein-Barr virus nuclear antigen (EBNA)-1. Mass cultures were selected in media containing G418 and puromycin. Serum-free conditioned media were concentrated in a dialysis bag with polyethylene glycol, dialyzed, and purified on Ni-NTA resin eluted with 250 mM imidazole. Purity was checked by silver staining or colloidal Coomassie blue staining [18].

Preparation of the secreted proteins

After incubation, the conditioned medium from the plates (12 h: 28×10^6 cells; 24 h: 50.5×10^6 cells) was carefully removed and centrifuged at 800 g at 4 °C for 10 min to remove suspended cells. PMSF (1 mM) was added to minimize enzymatic activity, and the medium was stored at −80 °C until analysis. As control the same amount of serum free medium, never been in contact with cells, and maintained 24 h at 37 °C in a humidified atmosphere containing 5% CO_2, was used. The cells were still 90–100% viable after the serum free growth as determined by trypan blue exclusion counting. After collecting the conditioned medium, the cell number was determined with a hemocytometer after detaching the cells with trypsin. The analyzed proteins were normalized to the same cell number or to a gel run in parallel and silver stained. The conditioned medium was dialyzed against 20 mM phosphate buffer, pH 7.4, in Spectra/Por CE dialysis tubing (Spectrum Laboratories, Breda, The Netherlands), 3.5–5 k MWCO, 31 mm flat width. HiTrap Q XL anion exchange column (GE Healthcare, Uppsala, Sweden) was then used to concentrate proteins from the conditioned medium. The HiTrap Q, connected to a peristaltic pump, was equilibrated with 20 mM phosphate buffer, pH 7.4 at 0.8 ml/min. The protein sample was loaded onto the cartridge at 0.8 ml/min, and then washed with the same buffer to elute salts from the cartridge while retaining the analyte. The proteins were eluted with 6 ml of 1 M NaCl in 20 mM phosphate buffer, pH 7.4 and then dialyzed and concentrated using Amicon® Ultra-4 centrifugal filter devices (cut off 3 kDa) (Millipore, Carrigtwohill, Ireland). The collected proteins were subjected to precipitation with cold acetone, resolubilized into buffer containing 7 M urea, 2 M thiourea and analyzed by SDS-PAGE. The bands were stained with Coomassie R350.

Western blotting

Protein extracts were separated on SDS/10% (w/v) polyacrylamide gel. Ten or twenty micrograms of proteins were transferred to nitrocellulose or to PVDF membranes (Schleicher and Schuell Bioscience) for the detection of progranulin. Western blots were carried out as already reported [8,9,19]. The antibodies used were the following: anti-granulins precursor polyclonal antibody and anti-ERK2 (Santa Cruz Biotechnology, Santa Cruz, CA, USA), anti-pERK1/2 (Cell Signaling Technology, Beverly, MA, USA), anti HSP70 (Affinity BioReagents, Golden, CO, USA, which detects different members of the HSP70 family including HSC70), anti HSP60 or anti ERp57 (Abcam, Cambridge, UK). pERK1/2 levels were normalized with respect to total ERK2 levels after incubation of the membrane with a stripping solution [8]. The blots were developed by the SuperSignal West Dura or the ECL procedure (Pierce Biotechnology, Rockford, IL, USA). Blots were quantified by Image Quant (Amersham Biosciences), after normalization to the same cell number.

Two-dimensional polyacrylamide gel electrophoresis

Thirty to 50 μg of total cell extracts were loaded onto 13 cm, pH 4–7 L IPG strips (GE Healthcare) in duplicate. IEF was conducted using an IPGPhor II system (GE Healthcare) according to the manufacturer's instructions. Focused strips were equilibrated with 6 M urea, 26 mM DTT, 4% w/v SDS, 30% v/v glycerol in 0.1 M Trisedronate–HCl (pH 6.8) for 15 min, followed by 6 M urea, 0.38 M iodoacetamide, 4% w/v SDS, 30% v/v glycerol, and a dash of bromophenol blue in 0.1 M Trisedronate–HCl, pH 6.8, for 10 min. The equilibrated strips were applied directly to 10% SDS-polyacrylamide gels and separated at 130 V. Gels were fixed and stained by Coomassie [20].

Evaluation of differentially represented spots

Gels were scanned with an Image Master 2-D apparatus and analyzed by the Melanie 5 software (GE Healthcare), which allowed estimation of relative differences in spot intensities for each represented protein. For each sample, three 2-DE gels were performed and then a comparative analysis was conducted [21]. Only the most significant differences were further investigated for identification by mass spectrometric analysis.

Sample preparation for mass spectrometric analysis

Spots from 2-DE were manually excised from the gel and dehydrated with acetonitrile. Proteins were then rehydrated in trypsin solution (Sigma Aldrich) and in-gel protein digestion was performed overnight at 37 °C. From each spot, 0.5 μL of the obtained peptides were spotted on the MALDI target, allowed to dry and then covered with 0.5 μL of the matrix solution α-cyano-4-hydroxycinnamic acid dissolved in acetonitrile 50% v/v and 0.1% SDS, the remaining volume was analyzed either by offline or online LCMS.

Offline liquid chromatography

Reversed-phase capillary HPLC was performed on a LC-2010 system (Shimadzu, Kyoto, Japan). Peptide solutions obtained by tryptic digestion of the 1-D and 2-D spots (1 μL) were prepared using 0.05% (v/v) aqueous TFA and loaded using a SIL-10A_{VP} autosampler (Shimadzu, Japan). Sample pre-concentration and desalting was accomplished using a Michrom Peptide CapTrap cartridge (0.5 mm (i.d.) × 2 mm) and components were separated on a Thermo Keystone Betabasic C_{18} column (0.32 mm (i.d.) × 10 mm). In gradient mode, the mobile phase composition was 0.1% (v/v) TFA for the aqueous phase and 0.1 (v/v) %TFA and acetonitrile (9:1 (v/v)) for the organic phase. LC-10AD_{VP} HPLC pumps (Shimadzu, Japan) were used to deliver solvent at a flow rate of 200 μL/min. The composition of %B was increased linearly for 50 min from 0% to 55%. Gradient profile was controlled by LC–MS Solution 2.0 Software. The UV response of the column eluent was monitored at a wavelength of 220 nm. The system was configured to perform a post-column split. The sample eluted with a flow rate of 5 μL/min was delivered to an online spotting robot system. Eluant was mixed with a saturated solution of α-cyano-4-hydroxycinnamic acid prepared in 50% (v/v) acetonitrile acidified with 0.1% (v/v) TFA. 10 spots of 1 μL each were deposited onto the MALDI target every minute.

MALDI mass spectrometry

All MALDI-ToF mass spectra were acquired on an Axima Resonance MALDI time-of-flight instrument (Shimazdu, Manchester, UK) equipped with a dual stage drift tube. Matrix-assisted laser desorption ionization of peptides was produced by pulses of UV light (λ = 337 nm, 3 ns pulse width) generated by a nitrogen laser with a maximum pulse rate of 10 Hz. The ion source was typically held at 1×10^{-6} mBar. Spectra were collected in reflectron mode using a delayed extraction of 145 ns. The accelerating voltage was set to +20 kV. The reflectron voltage was set to +25 kV. The detector (micro channel plate) was connected with a 1 GHz (8-bit) analog-to-digital converter. Spectra were the sum of 100 profiles on the same sample spot. Each profile was the result of two consecutive single laser pulses. The ToF was externally calibrated using an equimolar mixture of bradykinin, neurotensin and human adrenocorticotropic hormone ACTH 18–38. During data dependant MS/MS analysis, increase in the laser fluence was controlled at software level in order to augment the amount of internal energy imparted to the peptides on the spot ergo increase in fragmentation efficiency. Data analysis was performed using the

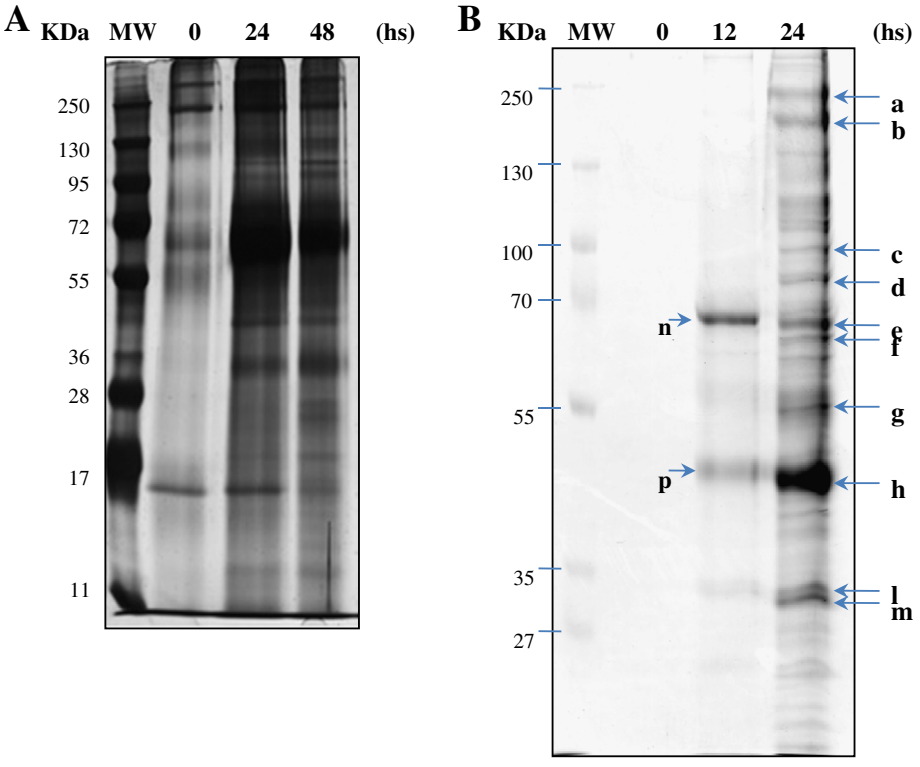

Fig. 1. Representative polyacrylamide gels of Hobit secreted proteins. A: Determination of optimal conditions for Hobit protein secretion. Supernatants from Hobit cells incubated in serum-free medium for the indicated times were fractionated, precipitated and analyzed by SDS-PAGE. Gel was silver-stained. B: 1D SDS-PAGE analysis of secreted protein. 60 μg (lane 3) and 100 μg (lane 4) of secreted proteins from Hobit cells was loaded on a 8% SDS-PAGE. Gel was stained with Coomassie blue. Arrow and letters indicate the bands analyzed by mass spectrometry, corresponding to that listed in Table 1. Approximate molecular mass (kDa) is also indicated.

Table 1
List of secreted proteins of Hobit osteoblastic cells, as detected by SDS-PAGE and identified by peptide mass fingerprint analysis. The corresponding band, mascot position, protein description, accession number (SwissProt entry), the experimental molecular mass, peptides detected and the associated score are listed. The unique nineteen proteins which were not known to be secreted by osteoblasts are indicated in bold.

Lane	Mascot position	Protein identity	UniProtKB/Swiss-Prot entry	Mass	Peptides matched	Score
Band a	1	Nidogen-2 (NID2)	Q14112	151,299	20	155
	2	Collagen alpha-1(I) chain (COL1A1)	P02452	138,827	39	145
	3	**Thrombospondin 1 (THBS1)**	Q59E99	134,762	5	88
	4	**Filamin-A (FLNA)**	P21333	281,254	2	75
	5	C-type mannose receptor 2 (MRC2)	Q9UBG0	166,549	1	59
	6	Fibronectin splice variant A (FN1)	A6YID2	66,766	2	55
	7	Attractin (ATRN)	O75882	158,432	2	42
	8	**Collagen alpha-2(IV) chain (COL4A2)**	P08572	167,449	3	41
	9	Follistatin-related protein 1 (FSTL1)	Q12841	34,963	1	39
Band b	1	Collagen alpha-1(I) chain (COL1A1)	P02452	138,827	34	151
	2	Nidogen-1 (NID1)	P14543	136,367	12	81
	3	Collagen alpha-2(I) chain (COL1A2)	P08123	129,209	4	54
	4	**Peroxidasin homolog (PXDN)**	Q92626	165,170	1	52
	5	Collagen alpha-1(III) chain (COL3A1)	P02461	138,479	3	35
	6	Complement factor H	P08603	139,005	3	34
Band c	1	**Endoplasmin (HSP90B1)**	P14625	92,753	20	994
	2	Galectin-3 (LGALS3)	P17931	65,718	14	854
	3	Sulfhydryl oxidase 1 (QSOX1)	O00391	83,375	17	787
	4	Transitional endoplasmic reticulum ATPase (VCP)	P55072	90,005	13	516
	5	Elongation factor 2 (EEF2)	P13639	96,307	10	511
	6	N-acetylglucosamine-6-sulfatase (GNS)	P15586	62,880	4	209
	7	Glycogen phosphorylase, muscle form (PYGM)	P11217	97,621	4	157
	8	Aminopeptidase N (ANPEP)	P15144	99,213	4	134
	9	Golgi membrane protein 1 (GOLM1)	Q8NBJ4	45,373	2	76
	10	Granulin (GRN)	P28799	68,594	2	70
	11	Collagen alpha-1(I) chain (COL1A1)	P02452	99,010	2	68
	12	Alpha-N-acetylglucosaminidase (NAGLU)	P54802	72,426	1	65
	13	Vasorin (VASN)	Q6EMK4	64,977	2	64
	14	Extracellular matrix protein 1 (ECM1)	Q16610	62,301	3	59
	15	Cadherin-2 (CDH2)	P19022	94,343	3	126
Band d	1	Heat shock protein HSP 90-beta (HSP90AB1)	P08238	83,636	22	1390
	2	unnamed protein product	85072	15	771	
	3	Gelsolin (GSN)	P06396	86,096	11	613
	4	hypothetical protein DKFZp762H157.1	74163	7	412	
	5	Heat shock protein HSP 90-alpha (HSP90AA1)	P07900	35,760	9	366
	6	Threonine–tRNA ligase, cytoplasmic (TARS)	P26639	84,347	8	304
	7	**Putative heat shock protein HSP 90-beta 2 (HSP90AB2P)**	Q58FF8	49,407	3	291
	8	**Vitamin K-dependent protein S (PROS1)**	P07225	77,176	7	265
	9	Golgi membrane protein 1 (GOLM1)	Q8NBJ4	45,373	3	164
	10	unnamed protein product	7979	3	140	
	11	prepro-alpha1(I) collagen (COL1A1)	P02452	139,937	4	133
	12	Collagen alpha-1(I) chain (COL1A1)	P02452	140,036	4	133
	13	Endoplasmic reticulum mannosyl-oligosaccharide 1,2-alpha-mannosidase (MAN1B1)	Q9UKM7	76,230	3	127
	14	Fibulin-5 (FBLN5)	Q9UBX5	52,562	2	108
	15	Galectin-3-binding protein (LGALS3BP)	Q08380	66,243	2	90
	16	Sulfhydryl oxidase 1 (QSOX1)	O00391	83,375	4	90
Band e	1	Proactivator polypeptide (PSAP)	P07602	60,236	14	842
	2	Heat shock cognate 71 kDa protein (HSPA8)	P11142	71,125	9	499
	3	Lumican (LUM)	P51884	38,741	6	305
	4	Radixin (RDX)	P35241	68,677	7	268
	5	Tyrosine-protein kinase receptor UFO (AXL)	P30530	98,631	4	215
	6	CD44 antigen (CD44)	P16070	53,911	3	158
	7	Lactotransferrin (LTF)	P02788	79,961	3	150
	8	72 kDa type IV collagenase (MMP2)	P08253	73,325	4	143
	9	1,4-Alpha-glucan-branching enzyme (GBE1)	Q04446	80,842	3	134
	10	Annexin A6 (ANXA6)	P08133	76,201	4	128
	11	Dickkopf-related protein 3 (DKK3)	Q9UBP4	39,489	2	108
	12	**Stress-70 protein, mitochondrial (HSPA9)**	P38646	74,064	3	106
	13	Beta-hexosaminidase subunit alpha (HEXA)	P06865	56,660	3	91
	14	Galectin-3-binding protein (LGALS3BP)	Q08380	66,243	2	86
	15	Putative phospholipase B-like 2 (PLBD2)	Q8NHP8	65,928	3	81
	16	Inter-alpha-trypsin inhibitor heavy chain H2 (ITIH2)	P19823	107,169	2	73
	17	**EGF-containing fibulin-like extracellular matrix protein 1 (EFEMP1)**	Q12805	45,077	2	62
Band f	1	Heat shock cognate 71 kDa (HSPA8)	P11142	70,898	23	1630
	2	72 kDa type IV collagenase (MMP2)	P08253	73,882	20	1263
	3	Heat shock-related 70 kDa protein 2 (HSPA2)	P54652	70,021	10	810
	4	moesin, isoform CRA_b (MSN)	P26038	51,390	14	665
	5	Chain A, Crystal Structure Of The Moesin Ferm DomainTAIL DOMAIN Complex	P26038	34,462	10	546
	6	Tripeptidyl-peptidase 1 (TPP1)	O14773	61,248	10	476
	7	Beta-hexosaminidase subunit alpha (HEXA)	P06865	58,367	9	449
	8	Proactivator polypeptide (PSAP)	P07602	58,113	8	428
	9	Lumican (LUM)	P51884	38,429	7	384

Table 1 (*continued*)

Lane	Mascot position	Protein identity	UniProtKB/Swiss-Prot entry	Mass	Peptides matched	Score
Band f	10	Putative phospholipase B-like 2 (PLBD2)	Q8NHP8	65,472	7	260
	11	Heat shock 70 kDa protein 1-like (HSPA1L)	P34931	70,376	4	254
	12	Heat shock 70 kDa protein 6 (HSPA6)	P17066	71,028	3	229
	13	Heat shock 70 kDa protein 1A/1B (HSPA1A)	P08107	70,052	5	215
	14	Polyadenylate-binding protein 1 (PABPC1)	P11940	70,324	4	145
	15	CD44 antigen (CD44)	P16070	81,538	2	125
Band g	1	45 kDa calcium-binding protein (SDF4)	Q9BRK5	41,750	5	125
	2	Protein disulfide-isomerase A3 (PDIA3)	P30101	56,747	23	118
	3	Heat shock 70 kDa protein 13 (HSPA13)	P48723	51,895	6	70
	4	Reticulocalbin-1 (RCN1)	Q15293	38,866	7	63
	5	**Inosine-5′-monophosphate dehydrogenase 2 (IMPDH2)**	P12268	55,770	1	61
	6	Retinoblastoma binding protein 7 (RBBP7)	B0R0W4	46,363	4	59
	7	Collagen alpha-1(I) chain (COL1A1)	P02452	138,827	3	55
	8	Follistatin-related protein 1 (FSTL1)	Q12841	34,963	6	54
	9	**Pyruvate kinase isozymes M1/M2 (PKM2)**	P14618	57,900	2	52
	10	**Olfactomedin-like protein 3 (OLFML3)**	Q9NRN5	45,981	2	43
	11	Lumican (LUM)	P51884	38,405	9	35
Band h	1	SPARC	P09486	35,488	20	845
	2	**Pigment epithelium-derived factor (SERPINF1)**	P36955	46,572	9	454
	3	**Rab GDP dissociation inhibitor beta (GDI2)**	P50395	51,120	14	446
	4	Adenosylhomocysteinase (AHCY)	P23526	48,285	10	421
	5	Gamma-glutamyl hydrolase (GGH)	Q92820	36,363	7	384
	6	**Rab GDP dissociation inhibitor beta (GDI2)**	P50395	46,075	12	361
	7	**Cathepsin L1 (CTSL1)**	P07711	38,020	5	245
	8	**Elongation factor 1-gamma (EEF1G)**	P26641	50,460	6	224
	9	Cathepsin Z (CTSZ)	Q9UBR2	34,627	6	208
	10	**N-acetyllactosaminide beta-1,3-N-acetylglucosaminyltransferase (B3GNT1)**	O43505	47,575	4	117
	11	**Proliferation-associated protein 2G4 (PA2G4)**	Q9UQ80	44,155	2	110
	12	Isocitrate dehydrogenase [NADP] cytoplasmic (IDH1)	O75874	46,973	3	110
	13	**Elongation factor 1-alpha 1 (EEF1A1)**	P68104	50,469	5	97
	14	Cathepsin B (CTSB)	P07858	38,777	2	92
Band l	1	Collagen alpha-1(III) chain (COL3A1)	P02461	138,564	8	332
	2	prepro-alpha1(I) collagen (COL1A1)	P02452	139,937	7	324
	3	Collagen, type I, alpha 1 (COL1A1)	P02452	140,036	7	324
	4	Collagen alpha-1(III) chain (COL3A1)	P02461	36,430	7	279
	5	Collagen alpha-2(I) chain (COL1A2)	P08123	41,522	4	112
	6	**Vesicular integral-membrane protein VIP36 (LMAN2)**	Q12907	39,711	2	53
Band m	1	Collagen alpha-1(III) chain (COL3A1)	P02461	139,809	21	1024
	2	Collagen alpha-2(I) chain (COL1A2)	P08123	41,864	14	713
	3	Collagen alpha-1(I) chain (COL1A1)	P02452	139,937	6	314
	4	Collagen alpha-1(I) chain (COL1A1)	P02452	140,036	6	314
	5	14-3-3 protein epsilon (YWHAE)	P62258	29,345	3	170
	6	**L-Lactate dehydrogenase A chain (LDHA)**	P00338	36,974	3	125
	7	**Fibrillin-1 (FBN1)**	P35555	332,906	2	87
Band n	1	Lactotransferrin (LTF)	P02788	78,078	2	134
	2	Heat shock cognate 71 kDa protein (HSPA8)	P11142	70,898	3	85
	3	Galectin-3-binding protein (LGALS3BP)	Q08380	66,243	2	77
	4	NXPE family member 2 (NXPE2)	Q96DL1	64,901	2	45
Band p	1	SPARC	P09486	34,610	20	64
	2	Cathepsin Z (CTSZ)	Q9UBR2	33,846	4	54
	3	Follistatin-related protein 1 (FSTL1)	Q12841	34,963	4	43
	4	Gamma-glutamyl hydrolase (GGH)	Q92820	35,941	3	36
	5	Collagen alpha-1(III) chain (COL3A1)	P02461	138,479	2	29

raw data. Protein identification was achieved using Mascot searching engine (Matrix Science) in conjunction with NCBInr database. The taxonomy selected was *Homo sapiens* and search parameters included: the selection of monoisotopic *m/z* values, a peptide mass tolerance of 0.2 Da, a peptide charge state of $^{+}1$ and a maximum number of missed cleavages of 2. Proteins were considered as identified if the Mascot score exceeded the significance threshold given by Mascot with at least 2 peptide identified for each protein listed as positive hit.

Online LC–MS

Tryptic digest samples were analyzed by LC–MS/MS using a NanoAcquity LC chromatographic system (Waters, Manchester, UK) coupled to a 4000 Q-TRAP (Applied Biosystems, Framingham, MA). Peptides were concentrated on a pre-column (20 mm × 180 μm i.d, Waters). The peptides were then separated using a gradient from 99% A (0.1% formic acid in water) and 1% B (0.1% formic acid in acetonitrile) to 30% B, in 40 min at 300 nL min^{-1}, using a 75 mm × 250 μm i.d. 1.7 μm BEH C18, analytical column (Waters). Peptides were selected for fragmentation automatically by data dependant analysis. Protein identifications were obtained by either Mascot Distiller or by our own in-house built software to generate peak lists that were suitable for submission to Mascot (Matrix Science). The generated peak lists were then submitted to Mascot for identification by MS/MS Ion search. Precursor ion tolerance was set at 1 Da and the MSMS ion tolerance at 0.5 Da. All other parameters were set as described in the MALDI section.

Gene annotations co-occurrence analysis

Gene IDs corresponding to the list of proteins identified by mass spectrometry analysis were submitted to GeneCodis (http://genecodis.cnb.csic.es/), a web-based tool for the ontological analysis, selecting *Homo sapiens* as the source for the annotations and Biological Process as Gene Ontology category to perform the gene annotation co-occurrence analysis.

Cell growth and survival assay

Hobit cells were cultured in 10% FBS supplemented DMEM-F12 until 60% of confluence, then were cultured in the same medium without serum in the absence or presence of 500 ng/ml progranulin (equivalent to ~6 nM). Determination of cell density and viability was carried out after 48 and 96 h by counting live and total cell densities with a hemocytometer using trypan blue exclusion assay. The overall experiment was repeated three times in triplicate. The percentage of live cell density was expressed over basal.

Apoptosis measurements

Apoptosis was assessed by staining of phosphatidyl-serines exposed on cell membranes with fluorescein isothiocyanate-labeled annexin V [22], according to manufacturer instructions (Roche Diagnostic Italia, Monza, Italy). Samples were analyzed by flow cytometry [23] using a Becton-Dickinson (Franklin Lakes, NJ) FACScan.

Statistical analysis

All experiments were performed with triplicate independent samples and were repeated at least twice, giving qualitatively identical results. Statistical analysis was performed using the Microsoft excel data analysis program for Student's *t*-test analysis. $P < 0.05$ was considered statistically significant.

Results

Secretome analysis by gel electrophoresis and mass spectrometry

In this work we carried out a comprehensive analysis of the secretome of human osteoblastic-like cells. To obtain a sufficient yield of protein samples for further MS analyses, it was important to choose a time of secretion that allowed maximal protein accumulation in the conditioned medium in association with minimal cell death. To this end, supernatants from Hobit cells incubated in serum-free medium for 0, 24 or 48 h and processed as reported in Material and Methods were analyzed by SDS-PAGE analysis. The amount of proteins (about 50–100 μg of purified secreted proteins from 25×10^6 cells) in the conditioned medium did not significantly change from 24 to 48 h of incubation (Fig. 1A), indicating that there was no appreciable protein degradation during this time interval. Cell viability after 24 h and 48 h incubation, in serum-free medium, was evaluated by MTT and trypan blue exclusion assays. The data showed no significant changes when the results were compared to cells incubated with complete medium (data not shown). The conditioned medium of the osteoblast-like cell line Hobit was analyzed by SDS-PAGE followed by protein identification by mass spectrometry. For this purpose, samples derived from the medium of the cells after 0, 12 h and 24 h of culture, were separated on SDS 8% (w/v) polyacrylamide gel (Fig. 1B).

The protein bands indicated by the arrows (Fig. 1B) were excised from the gel and subjected to in-gel trypsin digestion. With respect to a previous proteomics study performed in our laboratory [19], we opted for one dimensional gel electrophoresis due to the theoretical lesser number of proteins present in the secretome so that in principle a better protein recovery could be obtained. The tryptic peptide mixtures extracted from each individual one dimensional gel bands were subsequently analyzed by reversed phase liquid chromatography mass spectrometry. A total of 89 proteins were identified following MS analysis of all 12 gel band (Table 1). Among the identified species 19 were not known to be secreted by osteoblastic cells. As expected, the best protein recovery was found in gel bands of those samples containing proteins ranging from 60 to 100 kDa. In agreement with a previous publication [24], the Hobit cells secrete proteins also found in the secretome of human stromal bone cells such as osteonectin, lumican, fibrillin-1 and nidogen-1 which, together with the collagen type I, play a direct role in bone formation.

In order to assess if the identified secreted proteins belonged to groups of genes with similar biological meaning, unsupervised hierarchical clustering was performed using GeneCodis [25–27] a web-based tool for singular and modular enrichment analysis that integrates different source of information (i.e. Gene Ontology annotations) by looking for frequent patterns in the space of

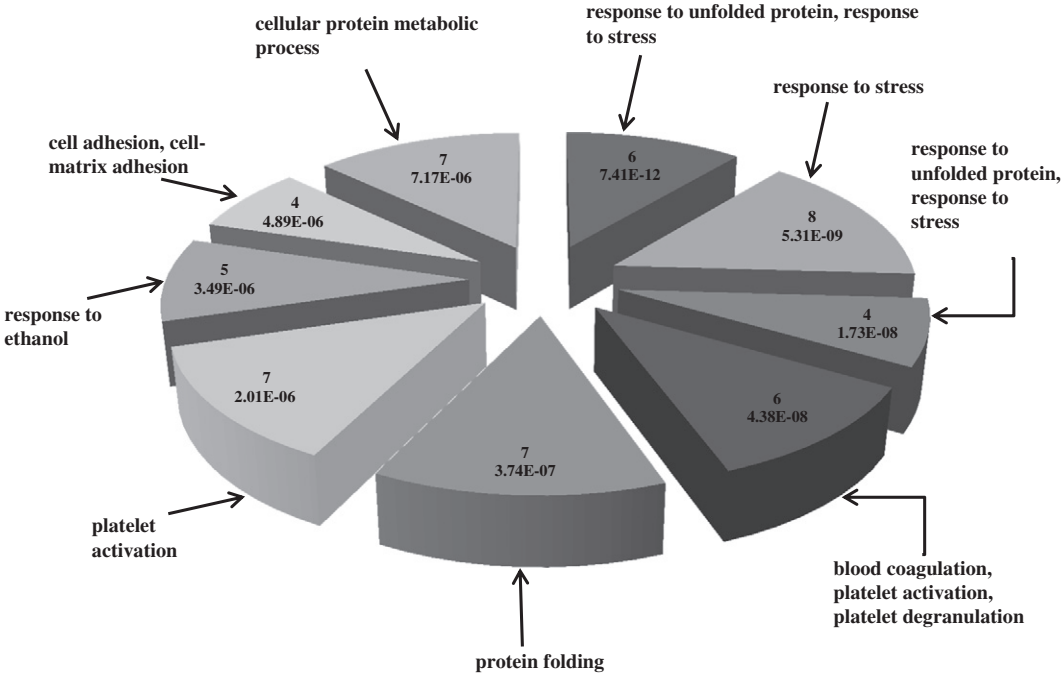

Fig. 2. Pie distribution of the functional enrichment analysis of the protein species identified by SDS-PAGE and mass spectrometry analysis clustered according to their biological process annotations. GeneCodis analysis of 89 unique identified secreted proteins. Only the most representative functional categories are represented. The number of genes belonging to each biological category and their statistical significance are provided on each label. See Table 1 in Supporting Information for the full list of annotations.

annotations and computing their statistical relevance (Fig. 2). This analysis allows dividing the identified proteins in clusters according to their biological process annotations (see Table 1 in Supporting Information). Through this functional enrichment analysis it has been pointed out that the secreted proteins found are mainly involved in cellular process such as response to stress, cell adhesion, cellular protein metabolic process and protein folding (Fig. 2).

The progranuline role

Among the identified proteins, we focused our attention on progranulin, which was previously detected also in the osteocytes proteome [9]. Progranulin has been shown to activate MAPK (ERK1/2) and PI3K signaling pathways in human multiple myeloma, breast, bladder and prostate cancer cells [13,14,28] and to promote cell growth, migration and invasion of human cancer cells through activation of ERK1/2 [11,28]. The relevance of this growth factor on osteoblast biology has never been studied.

Next, to validate the above described results, we performed Western immunoblotting analysis of the secreted proteins using a specific anti-human progranulin antibody. Twenty micrograms of proteins fractionated from Hobit secretome were separated onto 10% SDS-PAGE and immunoblotted. Progranulin was successfully detected in the medium after 24 h of incubation (Fig. 3A). Thus, based on these findings, we examined whether human recombinant progranulin would be able to trigger as signaling cascade in osteoblastic cells. To this end, we treated both MLO-Y4 and Hobit cells with progranulin (500 ng/ml, or ~6 nM) for 0–60 min. We found that both cell types responded to progranulin by inducing phosphorylation of ERK1/2 (Fig. 3B), albeit the cells differentially responded to the growth factor. As the ERK1/2 activation was more rapid and more intense in the osteocytes, we focused on these cells to the biological effects of progranulin on cell growth.

It is well established that activation of MAPK pathway leads to a positive effect on cell growth in osteoblastic cells [29,30]. The effect of exogenously-added progranulin on MLO-Y4 viability was examined by trypan blue exclusion assay. Treatment with 500 ng/ml progranulin (~6 nM) stimulated the osteocytic growth by 50% at 96 h (Fig. 3C), indicating that progranulin acts as an autocrine growth factor for these cells as well. Next, we determined whether progranulin could protect or counteract the pro-apoptotic activity of nutrient deprivation, i.e., serum-free conditions where sugar and salts are present but no serum proteins or growth factors/hormones are supplemented. Following a 24-h incubation in serum-free media, there was ~40% reduction of live cells (Fig. 4A). Exogenous progranulin at the same concentration as for the above experiments, was able to significantly rescue programmed cell death as shown by quantification of annexin V staining (Figs. 4 B and C). Although a small but significative increase in the percentage of necrotic cells after starvation is clearly apparent (from 4% in Basal, to 7% and 8% in St and St + P respectively, $p \leq 0.05$, *t* test compared to Basal), this percentage is much lower with respect to the percentage of apoptotic cells. Moreover, this increase was not reverted by progranulin treatment, suggesting that the progranulin efficiently prevent cell death due to apoptosis rather than to necrosis.

Collectively, these results indicate that progranulin is a pro-survival factor for osteocytes and could potentially play a direct role in bone growth and homeostasis.

We have previously demonstrated that the synthesis and secretion of endogenous progranulin in MLO-Y4 cells was induced by risedronate treatment (100 nM) [9]. The fact that also the osteoblastic-like cells may secrete this growth factor in the medium under basal conditions (cfr. Figs. 1B and 3A), prompted us to investigate whether risedronate treatment would also increase progranulin levels. To this end, serum-free conditioned medium from Hobit cells treated with 100 nM risedronate for the indicated time points was processed as described before and the expression of progranulin was evaluated by Western blot analysis (Fig. 5). Notably, there was a time-dependent induction of progranulin levels which peaked at 36 h, but remained significantly elevated at 48 h (Fig. 5).

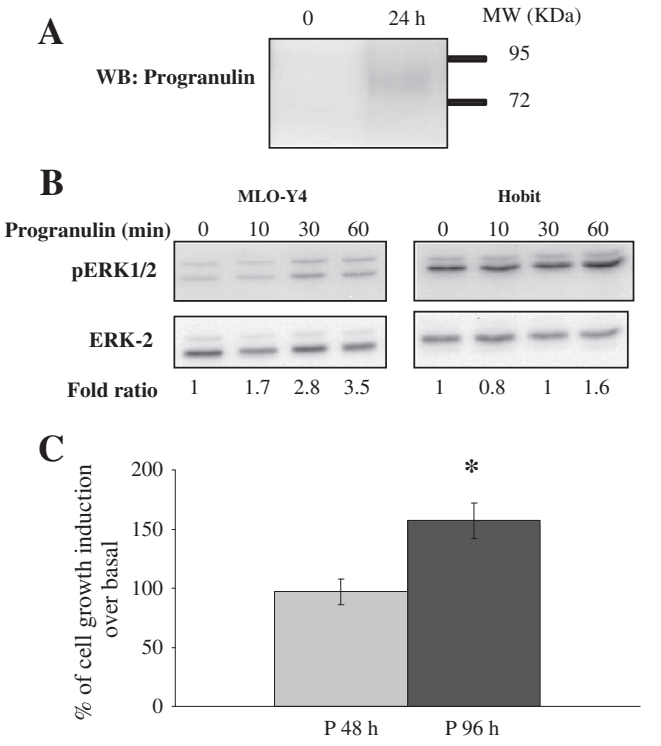

Fig. 3. Western blot confirmation of progranulin secreted by Hobit cells and progranulin effects on MLO-Y4 cells. A: Validation of the LC–MS identified progranulin by Western blot in Hobit secreted medium. The fractionated secreted medium was loaded in a 10% sodium dodecyl sulfate polyacrylamide gel, blotted and incubated with the specific primary antibody and horseradish peroxidase-conjugated secondary antibody. The analyzed proteins were normalized to a gel run in parallel and silver stained (data not shown). B: Effect of progranulin on phosphorylation of MAP kinase in MLO-Y4 and Hobit cells. Ten micrograms of protein derived from total cell lysates from cells treated with 500 ng/ml progranulin (~6 nM) for the indicated times, were loaded per lane and blotted with antiphospho-MAP kinase antibody. The same membrane was stripped and probed with anti-MAP kinase-2 antibody to examine equal loading. The MLO-Y4 cells were cultured in serum-free medium supplemented with 2% BSA, then progranulin was added for the indicated times. The Hobit cells were cultured in serum-free medium for 48 h, then progranulin was added to the culture medium for the indicated times. C: progranulin promotes MLO-Y4 cell growth. The number of live cells was measured by trypan blue exclusion assay from three independent experiments. P 48 h and P 96 h: cells maintained in presence of serum supplemented with 500 ng progranulin for 48 h and 96 h respectively. Data are expressed as fold of induction with respect to their relative basal condition. (*: $p \leq 0.05$ over basal).

Differentially-expressed protein species isolated by 2-DE analysis

To identify secreted proteins differentially regulated by risedronate, we performed a differential proteomic analysis of Hobit cell extracts by 2-DE. Comparison of the 2-DE maps of the secreted proteins from Hobit cells ± risedronate (100 nM for 48 h) is reported in Fig. 6A. To generate the secretome maps, the proteins were separated by 2-DE gels over the pI range 4–7, the most representative range in terms of species' abundance. Silver staining analysis of the gels allowed visualization of numerous resolved spots; among these, we selected those that showed a significant quantitative difference under treatment. In particular, three spots (Fig. 6B) were successfully matched among three sets of experiments, which displayed detectable differences with respect to basal untreated cells after analysis using the imaging Melanie 5 software (Spot #1: Treated/Basal: 1.7; Spot #2: Treated/Basal: 1.3; Spot #3: Treated/Basal: 1.5).

Utilization of tandem mass spectrometry following nanobore online liquid chromatography allowed the identification of the differentially

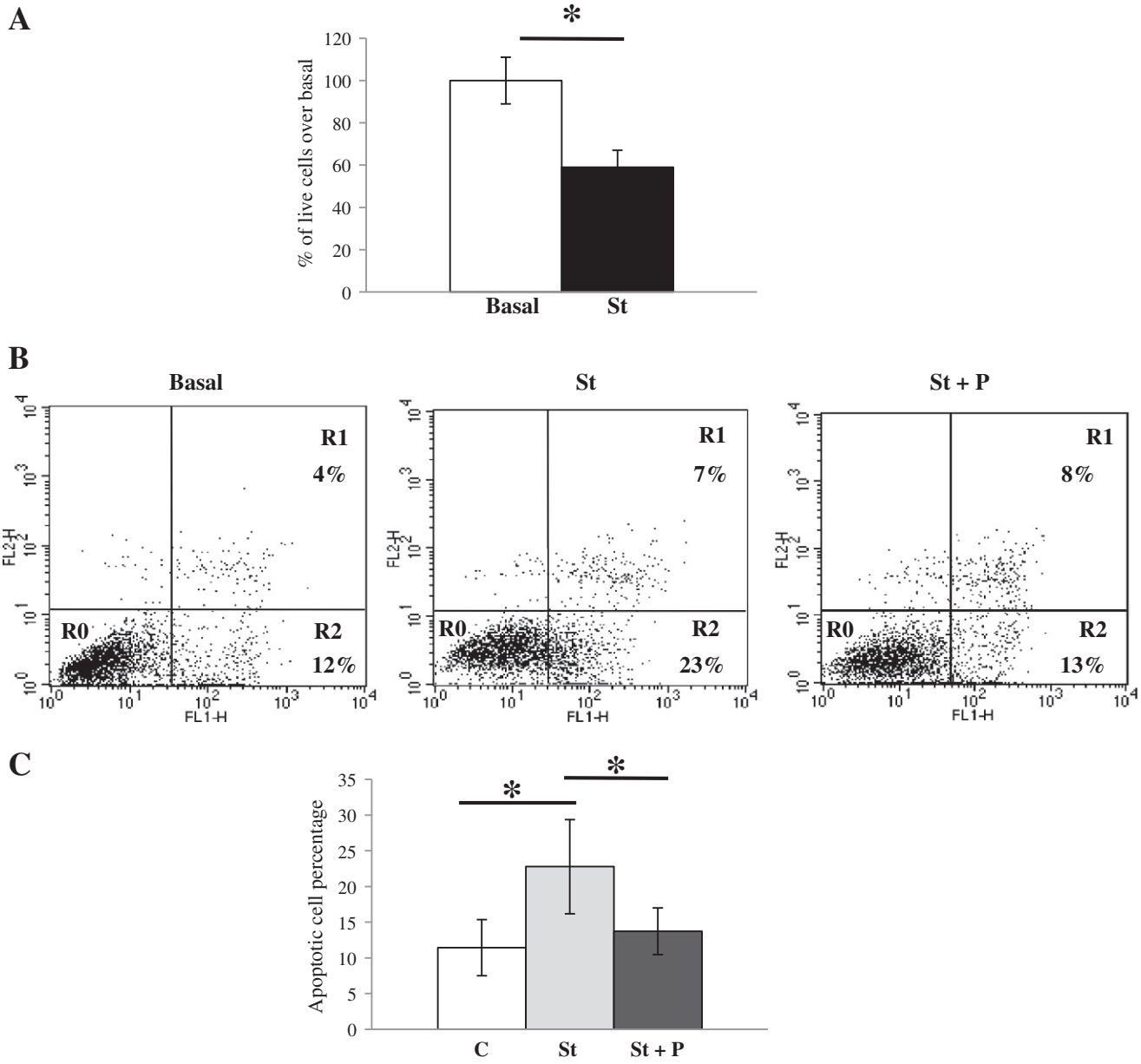

Fig. 4. Effect of progranulin on MLO-Y4 cells survival. A: MLO-Y4 were maintained in serum supplemented medium until confluence, live cell number were determined after other 24 h in presence (Basal) or absence (St) of serum. B: Representative FACS analysis of apoptotic MLO-Y4 cells after staining with Annexin-V-FLUOS and propidium iodide. MLOY4 cells were cultured in serum supplemented medium for 4 days in absence (C and St) or presence (St + P) of 500 ng/ml progranulin; cells were then maintained for 24 h in serum-free medium in absence or presence of the same concentration of progranulin. St: starved cells; St + P: starved cells in presence of 500 ng/ml progranulin. FL1: Annexin-V-FLUOS; FL2: propidium iodide. Cluster R0: living cells; R1: necrotic cells; R2: apoptotic cells. C: The Annexin-V_FLUOS results were expressed as means; bars ± SD. (*: $p \leq 0.05$, *t* test).

expressed species. The identified proteins, whose expression levels were induced after the treatment, were two heat shock proteins, HSC70 and HSP60, and Erp57, a disulfide isomerase. We further validated these results by Western blot analysis of the same conditioned media, by using specific antibodies. In all cases (i.e., HSC70, HSP60 and the ERp57), Western blotting data were in good agreement (Fig. 6C) with the expression pattern reported by MS analysis. To the best of our knowledge, this is the first time that these proteins have been found to be secreted by osteoblastic cells.

Discussion

The main function of osteoblastic cells is to manufacture bone through secretion of a large number of extracellular collagenous and non-collagenous proteins as well as mediators of bone mineralization. Indeed, osteoblasts can synthesize and secrete a large number of growth factors and cytokines that control osteoclastic bone resorption [31] and support hematopoiesis [32]. In addition, osteoblastic cells interact with the immune system through secretion of immune modulatory factors [33] and participate in overall energy metabolism through secretion of circulating factors, e.g. osteocalcin [5].

Hobit cells, a line derived from normal adult human osteoblastic cells transfected with the T-antigen of the SV40 virus, retain most of the osteoblastic differentiation markers, including the expression of osteocalcin, alkaline phosphatase, type I collagen, osteopontin 1α, and the sensitivity to steroid hormones [34]. The term "secretome" refers to proteins released through classical as well as nonclassical secretory pathways [35]. In addition, it also includes intracellular proteins that might be released through an active mechanism involving lysosomal vesicles and lipid rafts [36,37]. In this study we identified a

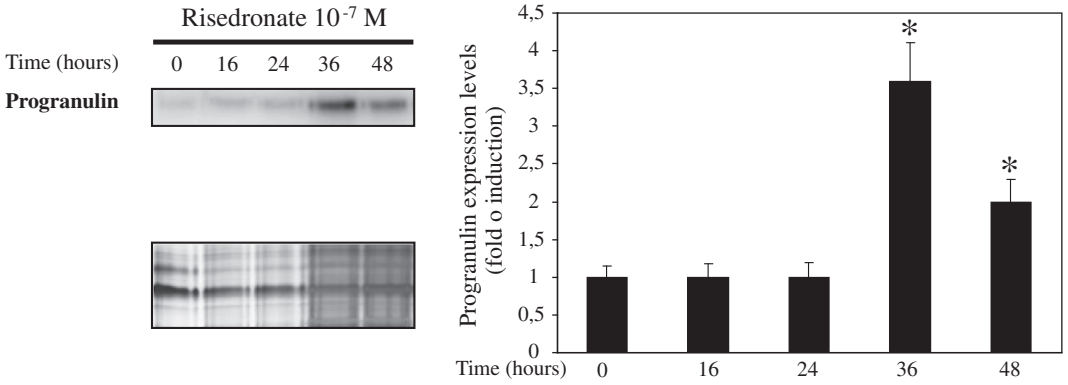

Fig. 5. Time course expression of progranulin in Hobit secretome after treatment with risedronate (100 nM). Representative Western blot analysis is reported. Right panel: values obtained from densitometric analysis of three independent experiments were reported as histograms. Columns represent progranulin protein levels normalized to a silver-stained lower portion of the gel (lower left panel). Columns and bars indicate the means ± SD for three independent experiments.(*: $p \leq 0.05$, *t* test, compared to non treated cells).

total of 89 proteins (19 unique to this study) which are involved in several biological processes including response to stress, cellular protein metabolic processes and protein folding (Fig. 2). In addition, we have strengthened the biological relevance of our findings by studying one of the identified factors: progranulin. We show here, for the first time, that progranulin is released in the medium by human Hobit osteoblastic cells. This soluble factor is an ~85 kDa glycoprotein corresponding to the precursor of the 6 kDa double-cysteine rich polypeptides called epithelins or granulins [10]. Moreover, similar to what previously found for progranulin in human breast cancer cells [13], mouse embryo fibroblast R-cells [38], SW.13 [39], multiple myeloma cells [14], and bladder cancer cells [16–18], we observed that exogenous progranulin induces MAP kinase phosphorylation, both in osteocytic- and in osteoblast-like cells. Thus, our findings indicate that osteoblasts also possess the signaling receptor for progranulin, which is still unknown, and further suggest that the MAPK pathway is shared by multiple cells with a wide histogenetic origin but that collectively respond to progranulin in an autocrine and paracrine fashion.

We provide evidence that exogenously added progranulin exerts proliferative and pro-survival effects in osteocytes. In the adult skeleton, osteocytes make up >90–95% of all bone cells compared with 4–6% osteoblast and 1–2% osteoclast. These cells are regularly dispersed throughout the mineralized matrix, connected to each other and to cells on the bone surface through dendritic processes generally radiating toward the bone surface and the blood supply. Osteocytes are thought to function as a network of sensory cells communicating with each other and with cells on the bone surface and the bone marrow [40]. Considerable experimental evidence is accumulating showing that osteocytes may control bone remodeling via direct cell-to-cell contacts and by soluble factors [41,42], several of them still unidentified. The progranulin found in the secretome of bone cells might therefore represent one of the factors that contribute to the mechanisms of communication within the osteocytic syncytium.

A large number of genes have been identified as possible candidates for the regulation of bone mass and susceptibility to osteoporotic fractures [43]. Among them are some of endoplasmic reticulum (ER) stress transducers which could play an important role in type I collagen synthesis and secretion. In fact, the development of osteoporosis correlates with ER stress response in osteoblasts of osteoporotic patients [44,45].

Our finding that osteoblasts progranulin secretion is potentiated by risedronate treatment is consistent with our previous data [9]. Moreover the differential proteomic study at the secretome level enabled us to identify three protein species spread over a pI range of 4–7 units, whose expression was induced after by risedronate: HSC70, HSP60 and ERp57. ERp57, a protein disulphide isomerase, is specifically expressed within the endoplasmic reticulum; however, in some cells, thiol isomerases are released and re-associate with the cell surface where they modulate a range of cellular functions, such as integrin-mediated adhesion, aggregation and granule secretion in platelets [46,47]. ER molecular chaperones such as BiP (immunoglobulin heavy-chain binding protein) and PDI (protein-disulfide isomerase) are induced in response to ER stress. BiP serves to restore folding of misfolded or incompletely-assembled proteins [44,45] and expression of BiP protects against various types of cell death induced by ER stress [48,49]. Moreover, it has been recently reported that both PDI and BiP are down-regulated in osteoblasts from osteoporosis patients and treatment of a murine model for osteoporosis with BIX, an inducer of BiP, could prevent bone loss through the activation of folding and secretion of bone matrix proteins [50]. Thus, risedronate-evoked expression of the protein-disulfide isomerase Erp57 could constitute a plausible alternate mechanism of action of aminobisphosphonates.

The heat shock proteins were long thought to be cytoplasmic proteins with functions restricted to the intra-cellular compartment. However, an increasing number of observations show that they can be released through physiological secretion mechanisms, bind to the surfaces of adjacent cells and then have a wide variety of bioactivities, such as promoting the survival of cells under stressful conditions [37,51–53]. In particular, Hsp60 (a group of mitochondrial chaperones) and Hsp70 are able to enter the blood stream and possess the ability to act at distant sites in the body and initiate signal transduction cascades [54]. These data reinforce our previous results [9], in which the comparative analysis of the proteome from MLO-Y4 treated with risedronate revealed the induction of the expression levels of molecular chaperones, as the 60 kDa heat shock protein, calreticulin and GRP78.

Conclusions

This is the first proteomic study providing a profile of the secretome of Hobit osteoblastic-like cells in which we identified 89 proteins species, 19 of which were not known to be secreted by osteoblastic cells. The majority of all previously reported protein constituents of human stromal stem cells were found [24], confirming our cellular model is suitable to study the osteoblasts biological processes. Among the identified proteins, we show here for the first time that progranulin exerts proliferative and pro-survival effects on osteocyte-like cells, suggesting that this growth factor merits further investigation in the context of osteoblast/osteocyte biology. Furthermore, our findings that risedronate upregulates the synthesis and secretion of progranulin together with the concurrent induction of ERp57, HSP60, HSC70, are novel and of biological significance. Indeed, the latter three proteins have been already shown to be associated with the promotion of cell

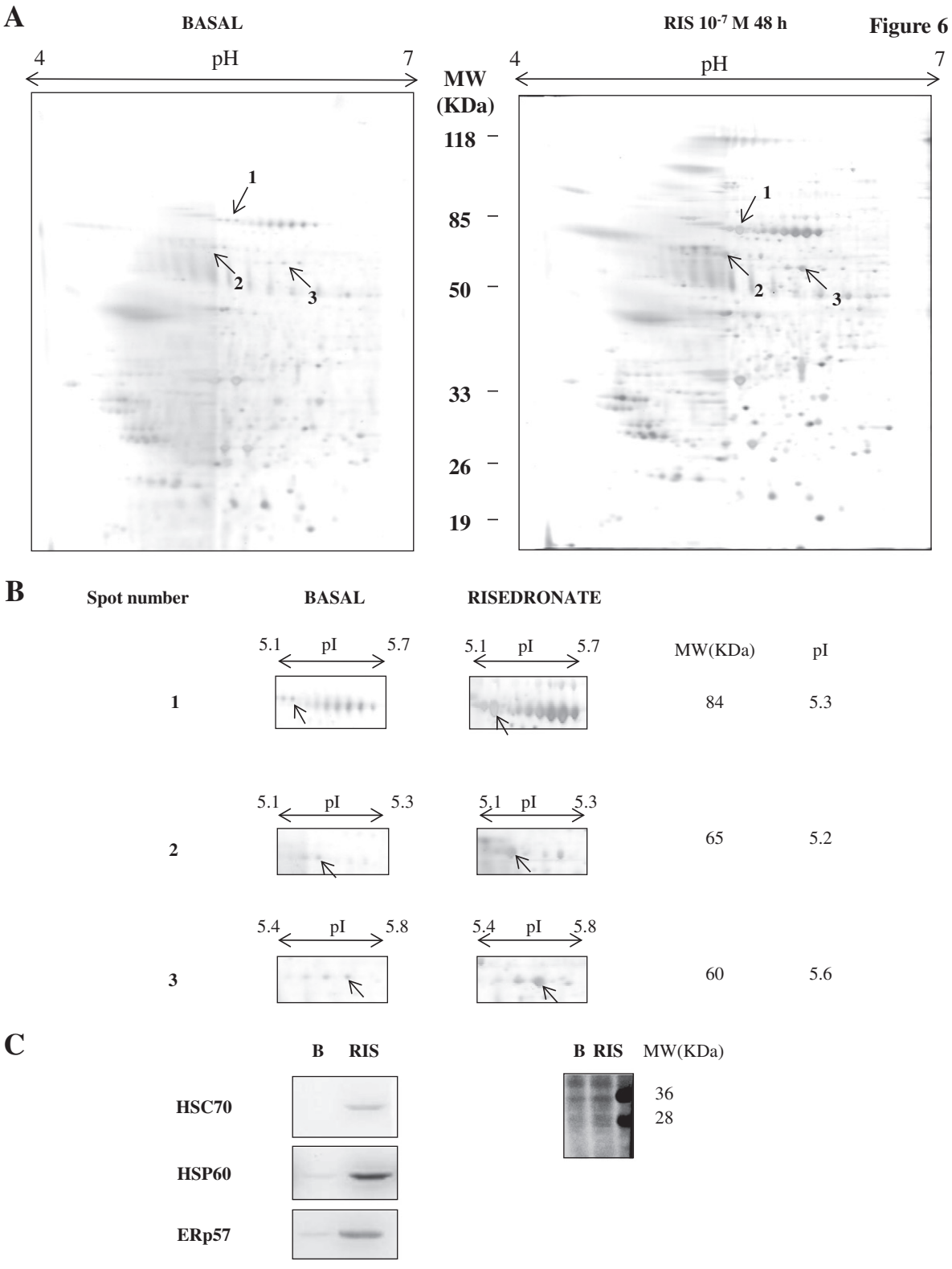

Fig. 6. Proteome maps of proteins secreted by Hobit cells. A: 2-DE proteome map of Hobit osteoblast-like cells after 48 h of treatment with risedronate 10^{-7} M. Samples containing 30–50 μg of secreted proteins were separated according to pI using 13-cm IPG strips (pI range 4–7), followed by a 10% SDS-PAGE. Arrows and numbers indicate the identified species. B: Differentially expressed species after 48 h of stimulation with risedronate (100 nM) indicated with numbers, as reported in A. Samples containing 30–50 μg of fractionated secreted proteins were prepared in rehydration buffer, separated according to pI using 13-cm IPG strips, pI range 4–7 and then loaded on a 10% SDS-PAGE. C: Validation by Western blot analysis of differentially expressed species from 2-DE gels approach (left). The blotted membrane stained by Ponceau was used as loading control (right). B: basal; RIS: risedronate (100 nM). M 48 h.

survival under stressful conditions and to prevent bone loss in osteoporosis by restoring folding of poorly-assembled bone matrix proteins [37,50]. Our collective results put forward progranulin as a novel player in bone response to stress and suggest that the molecular mechanisms of action of this class of compounds (i.e. bisphosphonates and alike) may involve different and complex mechanisms of action.

Supplementary data to this article can be found online at http://dx.doi.org/10.1016/j.bone.2013.10.003.

Acknowledgments

Authors thank Dr. G. Tell, Department of Biomedical Sciences and Technologies, University of Udine, Italy, and Dr. M. Openshaw, Shimadzu Research Laboratory (Europe), Manchester, U.K. for critical reading of the manuscript; Dr. M. Deganuto, Department of Biomedical Sciences and Technologies, University of Udine, Italy, for technical assistance in flow cytometry analysis. This work was supported by grants from Procter & Gamble to MR.

References

[1] Raisz LG. Pathogenesis of osteoporosis: concepts, conflicts, and prospects. J Clin Invest 2005;115:3318–25.
[2] Socrates SE. Bisphosphonates for postmenopausal osteoporosis. In: Clifford JR, editor. Primer on the metabolic bone diseases and disorders of mineral metabolism. 7th ed. Washington, D.C.: American Society for Bone and Mineral Research; 2008. p. 237–41.
[3] Rogers MJ. From molds and macrophages to mevalonate: a decade of progress in understanding the molecular mode of action of bisphosphonates. Calcif Tissue Int 2004;75:451–61.
[4] Plotkin LI, Weinstein RS, Parfitt AM, Roberson PK, Manolagas SC, Bellido T. Prevention of osteocyte and osteoblast apoptosis by bisphosphonates and calcitonin. J Clin Invest 1999;104:1363–74.
[5] Plotkin LI, Lezcano V, Thostenson J, Weinstein RS, Manolagas SC, Bellido T. Connexin 43 is required for the anti-apoptotic effect of bisphosphonates on osteocytes and osteoblasts in vivo. J Bone Miner Res 2008;23:1712–21.
[6] Plotkin LI, Aguirre JI, Kousteni S, Manolagas SC, Bellido T. Bisphosphonates and estrogens inhibit osteocyte apoptosis via distinct molecular mechanisms downstream of extracellular signal-regulated kinase activation. J Biol Chem 2005;280:7317–25.
[7] Bellido T, Plotkin LI. Novel actions of bisphosphonates in bone: preservation of osteoblast and osteocyte viability. Bone 2010;49/1:50–5.
[8] Romanello M, Bivi N, Pines A, Deganuto M, Quadrifoglio F, Moro L, et al. Bisphosphonates activate nucleotide receptors signaling and induce the expression of Hsp90 in osteoblast-like cell lines. Bone 2006;39:739–53.
[9] Bivi N, Picotti P, Muller LN, Romanello M, Moro L, Quadrifoglio F, et al. Shotgun proteomics analysis reveals new unsuspected molecular effectors of nitrogen-containing bisphosphonates in osteocytes. J Proteomics 2011;74(7):1113–22.
[10] Lu R, Serrero G. Stimulation of PC cell-derived growth factor (epithelin/granulin precursor) expression by estradiol in human breast cancer cells. Biochem Biophys Res Commun 1999;256:204–7.
[11] Monami G, Gonzalez EM, Hellman M, Gomella LG, Baffa R, Iozzo RV, et al. Proepithelin promotes migration and invasion of 5637 bladder cancer cells through the activation of ERK1/2 and the formation of a paxillin/FAK/ERK complex. Cancer Res 2006;66:7103–10.
[12] Zhou J, Gao G, Crabb JW, Serrero G. Purification of an autocrine growth factor homologous with mouse epithelin precursor from a highly tumorigenic cell line. J Biol Chem 1993;268:10863–9.
[13] Lu R, Serrero G. Mediation of estrogen mitogenic effect in human breast cancer MCF-7 cells by PC-cell-derived growth factor (PCDGF/granulin precursor). Proc Natl Acad Sci U S A 2001;98:142–7.
[14] Wang W, Hayashi J, Kim WE, Serrero G. Cell-derived growth factor (granulin precursor) expression and action in human multiple myeloma. Clin Cancer Res 2003;9:2221–8.
[15] Wang W, Hayashi J, Serrero G. PC cell-derived growth factor confers resistance to dexamethasone and promotes tumorigenesis in human multiple myeloma. Clin Cancer Res 2006;12:49–56.
[16] Gonzalez EM, Mongiat M, Slater SJ, Baffa R, Iozzo RV. A novel interaction between perlecan protein core and progranulin: potential effects on tumor growth. J Biol Chem 2003;278:38113–6.
[17] Lovat F, Bitto A, Xu SQ, Fassan M, Goldoni S, Metalli D, et al. Proepithelin is an autocrine growth factor for bladder cancer. Carcinogenesis 2009;30:861–8.
[18] Mongiat M, Sweeney S, San Antonio JD, Fu J, Iozzo RV. Endorepellin, a novel inhibitor of angiogenesis derived from the carboxyl terminus of perlecan. J Biol Chem 2003;278:4238–49.
[19] Bivi N, Bereszczak JZ, Romanello M, Zeef LAH, Delneri D, Quadrifoglio F, et al. Transcriptome and proteome analysis of osteocytes treated with nitrogen-containing bisphosphonates. J Proteome Res 2009;8(3):1131–42.
[20] Candiano G, Bruschi M, Musante L, Santucci L, Ghiggeri GM, Carnemolla B, et al. Blue silver: a very sensitive colloidal Coomassie G-250 staining for proteome analysis. Electrophoresis 2004;25:1327–33.
[21] Vascotto C, Cesaratto L, Zeef LA, Deganuto M, D'Ambrosio C, Scaloni A, et al. Genome-wide analysis and proteomic studies reveal APE1/Ref-1multifunctional role in mammalian cells. Proteomics 2009;9:1058–74.
[22] Vermes I, Haanen C, Steffens-Nakken H, Reutelingsperger C. A novel assay for apoptosis. Flow cytometric detection of phosphatidylserine expression on early apoptotic cells using fluorescein labelled Annexin V. J Immunol Methods 1995;184:39–51.
[23] Homburg CH, de Haas M, von dem Borne AE, Verhoeven AJ, Reutelingsperger CP, Roos D. Human neutrophils lose their surface Fc gamma RIII and acquire Annexin V binding sites during apoptosis in vitro. Blood 1995;85:532–40.
[24] Kristensen LP, Chen L, Overbeck Nielsen M, Qanie DW, Kratchmarova I, Kassem M, et al. Temporal profiling and pulsed SILAC labeling identify novel secreted proteins during *ex vivo* osteoblast differentiation of human stromal stem cells. Mol Cell Proteomics 2012;11(10):989–1007.
[25] Tabas-Madrid D, Nogales-Cadenas R, Pascual-Montano A. GeneCodis3: a non-redundant and modular enrichment analysis tool for functional genomics. Nucleic Acids Res 2012;40:W478–83.
[26] Nogales-Cadenas R, Carmona-Saez P, Vazquez M, Vicente C, Yang X, Tirado F, et al. GeneCodis: interpreting gene lists through enrichment analysis and integration of diverse biological information. Nucleic Acids Res 2009;37:W317–22.
[27] Carmona-Saez P, Chagoyen M, Tirado F, Carazo JM, Pascual-Montano A. GENECODIS: A web-based tool for finding significant concurrent annotations in gene lists. Genome Biol 2007;8(1):1–8.
[28] Monami G, Emiliozzi V, Bitto A, Lovat F, Xu SQ, Goldoni S, et al. Proepithelin regulates prostate cancer cell biology by promoting cell growth, migration, and anchorage-independent growth. Am J Pathol 2009;174:1037–47.
[29] Mathov I, Plotkin LI, Sgarlata CL, Leoni J, Bellido T. Extracellular signal-regulated kinases and calcium channels are involved in the proliferative effect of bisphosphonates on osteoblastic cells in vitro. J Bone Miner Res 2001;16:2050–6.
[30] Hipskind RA, Bilbe G. MAP kinase signaling cascades and gene expression in osteoblasts. Front Biosci 1998;3:804–16.
[31] Kobayashi Y, Udagawa N, Takahashi N. Action of RANKL and OPG for osteoclastogenesis. Crit Rev Eukaryot Gene Expr 2009;19:61–72.
[32] Porter RL, Calvi LM. Communications between bone cells and hematopoietic stem cells. Arch Biochem Biophys 2008;473:193–200.
[33] Lorenzo J, Horowitz M, Choi Y. Osteoimmunology: interactions of the bone and immune system. Endocr Rev 2008;29:403–40.
[34] Keeting PE, Scott RE, Colvard DS, Anderson MA, Oursler MJ, Spelsberg TC, et al. Development and characterization of a rapidly proliferating, well-differentiated cell line derived from normal adult osteoblast-like cells transfected with SV40 large T antigen. J Bone Miner Res 1992;7:127–36.
[35] Volmer MW, Stuhler K, Zapatka M, Schoneck A, Klein-Scory S, Schmiegel W, et al. Differential proteome analysis of conditioned media to detect Smad4 regulated secreted biomarkers in colon cancer. Proteomics 2005;5:2587–601.
[36] Ireland HE, Leoni F, Altaie O, Birch CS, Coleman RC, Hunter-Lavin C, et al. Measuring the secretion of heat shock proteins from cells. Methods 2007;43:176–83.
[37] Evdokimovskaya Y, Skarga Y, Vrublevskaya V, Morenkov O. Secretion of the heat shock proteins HSP70 and HSC70 by baby hamster kidney (BHK-21) cells. Cell Biol Int 2010;34(10):985–90.
[38] Zanocco-Marani T, Bateman A, Romano G, Valentinis B, He ZH, Baserga R. Biological activities and signaling pathways of the granulin/epithelin precursor. Cancer Res 1999;59:5331–40.
[39] He Z, Ismail A, Kriazhev L, Sadvakassova G, Bateman A. Progranulin (PC-cell-derived growth factor/acrogranin) regulates invasion and cell survival. Cancer Res 2002;62:5590–6.
[40] Bonewald LF. Osteocytes. In: Clifford JR, editor. Primer on the metabolic bone diseases and disorders of mineral metabolism. 7th ed. Washington, D.C.: American Society for Bone and Mineral Research; 2008. p. 22–7.
[41] Heino TJ, Hentunen TA, Vaananen HK. Osteocytes inhibit osteoclastic bone resorption through transforming growth factor-beta: enhancement by estrogen. J Cell Biochem 2002;85:185–97.
[42] Heino TJ, Hentunen TA, Vaananen HK. Conditioned medium from osteocytes stimulates the proliferation of bone marrow mesenchymal stem cells and their differentiation into osteoblasts. Exp Cell Res 2004;294:458–68.
[43] Ralston SH, de Crombrugghe B. Genetic regulation of bone mass and susceptibility to osteoporosis. Genes Dev 2006;20:2492–506.
[44] Yoshida H. ER stress and diseases. FEBS J 2007;274:630–58.
[45] Ni M, Lee AS. ER chaperones in mammalian development and human diseases. FEBS Lett 2007;581:3641–51.
[46] Jordan PA, Gibbins JM. Extracellular disulfide exchange and the regulation of cellular function. Antioxid Redox Signal 2006;8:312–24.
[47] Holbrook LM, Watkins NA, Simmonds AD, Jones CI, Ouwehand WH, Gibbins JM. Platelets release novel thiol isomerase enzymes which are recruited to the cell surface following activation. Br J Haematol 2010;148:627–37.
[48] Katayama T, Imaizumi K, Sato N, Miyoshi K, Kudo T, Hitomi J, et al. Presenilin-1 mutations downregulate the signalling pathway of the unfolded-protein response. Nat Cell Biol 1999;1:479–85.
[49] Rao RV, Peel A, Logvinova A, del Rio G, Hermel E, Yokota T, et al. Coupling endoplasmic reticulum stress to the cell death program: role of the ER chaperone GRP78. FEBS Lett 2002;514:122–8.
[50] Hino S, Kondo S, Yoshinaga K, Saito A, Murakami T, Kanemoto S, et al. Regulation of ER molecular chaperone prevents bone loss in a murine model for osteoporosis. J Bone Miner Metab 2010;28:131–8.
[51] Merendino AM, Bucchieri F, Campanella C, Marcianò V, Ribbene A, David S, et al. Hsp60 is actively secreted by human tumor cells. PLoS One 2010;5/2:e9247.
[52] Nirdé P, Derocq D, Maynadier M, Chambon M, Basile I, Gary-Bobo M, et al. Heat shock cognate 70 protein secretion as a new growth arrest signal for cancer cells. Oncogene 2010;29:117–27.
[53] Tytell M. Release of heat shock proteins (Hsps) and the effects of extracellular Hsps on neural cells and tissues. Int J Hyperthermia 2005;21:445–55.
[54] Calderwood SK, Mambula SS, Gray Jr PJ, Theriault JR. Extracellular heat shock proteins in cell signaling. FEBS Lett 2007;581:3689–94.